

DanceAnyWay: Synthesizing Mixed-Genre 3D Dance Movements Through Beat Disentanglement

Aneesh Bhattacharya^{*1,3}, Uttaran Bhattacharya², and Aniket Bera³

¹International Institute of Information Technology, Naya Raipur, Chhattisgarh, India

²Adobe Research, San Jose, California, USA

³Purdue University, West Lafayette, Indiana, USA

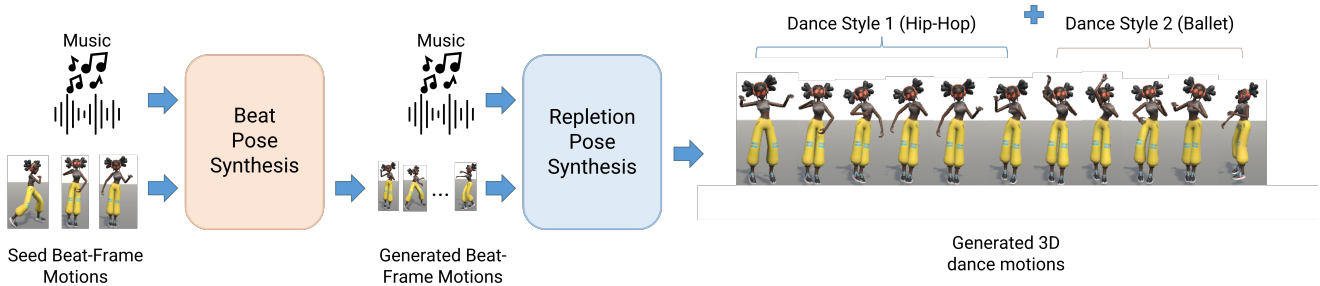


Figure 1: **DanceAnyWay**. A two-stage hierarchical network that can generate diverse, mixed-genre 3D dance motions with global translations given music or song audio. We render our results with Mixamo characters [34].

Abstract

We present *DanceAnyWay*, a hierarchical generative adversarial learning method to synthesize mixed-genre dance movements of 3D human characters synchronized with music. Our method learns to disentangle the dance movements at the beat frames from the dance movements at all the remaining frames by operating at two hierarchical levels. At the coarser “beat” level, it encodes the rhythm, pitch, and melody information of the input music via dedicated feature representations only at the beat frames. It leverages them to synthesize the beat poses of the target dance using a sequence-to-sequence learning framework. At the finer “repletion” level, our method encodes similar rhythm, pitch, and melody information from all the frames of the input music via dedicated feature representations and couples them with the synthesized beat poses from the coarser level to synthesize the full target dance sequence using an adversarial learning framework. By disentangling the broader dancing styles at the coarser level from the specific dance move-

ments at the finer level, our method can efficiently synthesize dances composed of arbitrarily mixed genres and styles. We evaluate the performance of our approach through extensive experiments on both the mixed-genre TikTok dance dataset and the single-genre AIST++ dataset and observe improvements of about 2% in motion quality metrics and 1.6% – 5.9% in motion diversity metrics over the current baselines in the two datasets respectively. We also conducted a user study to evaluate the visual quality of our synthesized dances. We noted that, on average, the samples generated by our method were about 9% more preferred by the participants and had a 12% better five-point Likert-scale score over the best available current baseline in terms of motion quality and diversity.

1. Introduction

Dancing is a central human behavior observed across the divides of society and culture [26]. It is simultaneously a form of expression and communication, due to which dance videos have become some of the most popular content in modern social media [42]. Such social media dance videos

^{*}Work done while Aneesh was an intern at the IDEAS Lab, Purdue University

are most commonly created by amateurs and aspiring professionals [10]. Their dances are often improvised and therefore contain a seemingly random mixture of various dancing styles that do not conform to any particular dance genre. As a result, it is extremely challenging to develop automated techniques to reliably generate such dances for use in large-scale computer graphics and AR/VR applications such as character design [32], storyboard visualization for consumer media [25, 45], and creation of large-scale VR worlds such as the metaverse [37].

Learning-based approaches have attempted to capture the pattern of the more conventional single-genre dances to generate dance motions but suffer from issues such as temporal conflicts [11] and motion freezing and instability [29], which are only exacerbated when applied to the problem of synthesizing mixed-genre dances. A common circumvention of these issues is to use seed poses [29, 49, 28] to enforce plausible movements. However, seed motions only provide the initial dance characteristics, which becomes insufficient over time for generating long dance sequences. By contrast, looking at the general structure of mixed-genre dances [20], our key observation is that dancers often exhibit sporadic bursts or drops of energy at the beats of the music. Therefore, knowing the dance steps at the beats of the music can help in predicting the entire dance by filling in the intermediate steps. In this paper, we introduce our method *DanceAnyWay* that follows this ideology to generate plausible, mixed-genre 3D dance sequences from music or song audio. We learn the correlation between the dance motions and the music at two temporal levels: a coarser *beat level*, which corresponds to the dance poses at the beat frames in the audio, and a finer *repletion level*, which corresponds to the dance poses at all the other frames in the audio. By explicitly learning the correlation between the audio and the dance poses at the beat frames, we can generate plausible beat pose sequences representing the underlying dance characteristics for the entirety of the music. Given these beat poses, we can generate the remaining or repletion poses adapting to the different dance styles in between the beat frames.

In summary, our main contributions are as follows:

- We propose a hierarchical learning method using sequence-to-sequence and generative adversarial learning to synthesize mixed-genre dance movements of 3D human characters synchronized with music.
- We leverage two different temporal representations of the music and its corresponding dance for the network, allowing us to ensure cohesion between the synthesized dance and coarse and fine features of the music.
- We utilize a spatial-temporal graph representation of the 3D human poses to capture the localized and macroscopic body movements throughout the dance and further use it to synthesize dances with greater har-

mony between the joint movements.

- We provide extensive evaluations and a comprehensive user study to evaluate our performance quantitatively and qualitatively for the generation of realistic single-genre and mixed-genre 3D dances.

2. Related Work

We briefly review prior work on 3D human motion synthesis, particularly from audio modalities such as speech and music as inputs.

3D Human Motion-to-Motion Synthesis 3D human motion-to-motion synthesis is a richly explored area in computer graphics and machine learning. Classical approaches have considered a variety of mathematical models such as kernel-based probability distributions [14, 38] to predict the most likely future poses given past poses, and motion graphs [4, 23] to represent poses as nodes in a graph and transitioning between those poses according to various linking rules to generate realistic motions. More recently, learning-based approaches such as those using CNNs [17, 18], RNNs [13, 2, 21, 15, 24, 9, 44, 8], GANs [39], GCNs [47] and transformers [1, 6] have led to state-of-the-art results on large-scale datasets. These methods generate 3D human motions into the future based on past motions and do not consider additional input modalities such as audio.

3D Dance Motion Synthesis from Music Motion Graph-based approaches are also used in music-to-dance synthesis by incorporating constraints on the linking rules based on the music rhythm [11, 40]. However, the generated dance motions often suffer from temporal conflicts due to the difference in tempos across dances. More recent approaches for generating 3D dance motions use LSTMs [43, 46], GANs [27, 40] and transformers [28, 29, 41] for large-scale synthesis. These methods benefit from the development and release of large-scale 3D dance datasets collected using mocap [3, 43, 49] and mapped to 3D human models [30]. Given the high dimensionality of long pose sequences, these methods can sometimes result in non-standard poses or regress to mean configurations without exhibiting animated movements. By contrast, our method explicitly learns beat poses at regular intervals in the sequence to both conform to standard poses and avoid regression to mean configurations.

3D Human Motion Synthesis from Other Modalities. Apart from music, 3D motion synthesis is also commonly performed based on other modalities, such as speech and text. For example, methods for co-speech gesture synthesis learn individual gesticulation patterns for personalized synthesis [16], use GAN-based approaches to improve plau-

sibility [12], and combine both of these approaches with additional signals such as the text transcript of speech [48] and leverage the emotional expressions through physiological variations in the gestures [5] for more robust and diverse synthesis. In our work, we similarly learn from the physiological variations in the dance movements and use a GAN-based architecture to improve the plausibility of the generated motions.

3. Generating Mixed-Genre 3D Dance Motions

Our goal is to generate 3D pose sequences for mixed-genre dances by learning the correlation between the music or song audio and the dance movements. To learn mixed-genre dance movements, our approach is to separately learn the *structure* of the dance described by the *beat poses* or the poses at the beat frames of the audio, and the *finer details* of the dance described by the *repletion poses* or the poses at the remaining frames. To this end, we develop a two-stage learning method consisting of Beat Pose Synthesis (BPS) followed by Repletion Pose Synthesis (RPS). In BPS, given a short sequence of seed beat poses and the audio, we generate the beat poses. In RPS, given all the seed poses, the beat poses following the seed pose duration, and the audio, we generate the remaining poses to complete the dance. Mathematically, we represent the pose at frame t as $\mathcal{U}_t = [u_t^{(1)}, \dots, u_t^{(J-1)}] \in \mathbb{R}^{(J-1) \times 3}$, consisting of the unit line vectors denoting the $J - 1$ bones corresponding to the J body joints. We take in the audio as a raw waveform and process it into a feature sequence $\mathcal{A} = [a_1, \dots, a_T] \in \mathbb{R}^{D_{\mathcal{A}} \times T}$ for some feature dimension $D_{\mathcal{A}}$ and total temporal length T . We extract the beat frames from the audio using available beat detection methods and represent them as a set $B = \{\text{beat frames in } \mathcal{A}\}$. Our BPS takes in the audio features \mathcal{A} and the initial seed beat pose sequence $\mathcal{U}_{B_S} = \{\mathcal{U}_f\}_{f \in B_S}$, where $B_S \subset B$ consists of all the beat frames in B contained within the seed sequence length $T_S \ll T$, and generates the beat poses corresponding to $\mathcal{U}_{-B_S} = \{\mathcal{U}_f\}_{f \in B - B_S}$. Our RPS takes in the audio features \mathcal{A} , all the seed poses $\mathcal{U}_S = \{\mathcal{U}_f\}_{f \in \{1, \dots, T_S\}}$, and the generated beat poses corresponding to $\mathcal{U}_{-B_S} = \{\mathcal{U}_f\}_{f \in -B_S}$, and synthesizes the repletion poses corresponding to $\mathcal{U}_R = \{\mathcal{U}_f\}_{f \in R}$ where $R = \{1, \dots, T\} - B$. We first fully train our BPS and then use its generated outputs to fully train our RPS. We show the overview of our end-to-end pipeline in Fig. 2 and describe the individual components below.

3.1. Beat Pose Synthesis

Our Beat Pose Synthesis (BPS) network has a sequence-to-sequence architecture consisting of an encoder and a decoder. The encoder takes in the raw audio waveform ψ of the input audio and the seed beat pose sequence \mathcal{U}_{B_S} and

combines them into a latent, beat-aware representation. The decoder takes in these latent representations and generates the beat poses $\hat{\mathcal{U}}_{-B_S}$.

3.1.1 Encoder

We encode the audio and seed pose sequences using separate encoder blocks. The *audio encoder block* consists of an MFCC encoder and a Chroma encoder. MFCCs naturally capture the human auditory response and are commonly used in tasks such as emotion recognition [36] and speaker identification [35]. In our work, we leverage the music prosody and the vocal intonations (when present) captured by the MFCCs. The MFCC encoder takes in the MFCCs and their first- and second-order derivatives and uses convolutional layers to learn D_M -dimensional latent feature sequences $\mathcal{A}_{M_{BEnc}} \in \mathbb{R}^{D_M \times |B|}$ from their localized inter-dependencies as

$$\mathcal{A}_{M_{BEnc}} = \text{MFCCEncoder}_{BEnc}(\text{MFCC}(\psi); W_{M_{BEnc}}), \quad (1)$$

where $W_{M_{BEnc}}$ denotes the trainable parameters. Chroma CENS features capture the melody and pitch in music, and we use the Chroma encoder with convolutional layers to transform these Chroma CENS features into $D_{C_{BEnc}}$ -dimensional latent feature sequences $\mathcal{A}_{C_{BEnc}} \in \mathbb{R}^{D_{C_{BEnc}} \times |B|}$ based on their localized inter-dependencies as

$$\mathcal{A}_{C_{BEnc}} = \text{ChromaEncoder}_{BEnc}(\text{Chroma}(\psi); W_{C_{BEnc}}), \quad (2)$$

where $W_{C_{BEnc}}$ denotes the trainable parameters. We concatenate these two features into our audio features \mathcal{A}_{BEnc} as

$$\mathcal{A}_{BEnc} = [\mathcal{A}_{M_{BEnc}}; \mathcal{A}_{C_{BEnc}}] \in \mathbb{R}^{D_{\mathcal{A}_{BEnc}} \times |B|}, \quad (3)$$

where $D_{\mathcal{A}_{BEnc}} = D_M + D_{C_{BEnc}}$. For the *pose encoder block*, we adopt the pose encoder architecture of [5] to learn the physiological variations in the dance motions represented by \mathcal{U}_{B_S} . The pose encoder block outputs latent pose features $\mathcal{P} \in \mathbb{R}^{D_{\mathcal{P}} \times |B|}$ as

$$\mathcal{P}_{BEnc} = \text{PoseEncoder}_{BEnc}(\mathcal{U}_{B_S}; W_{\mathcal{P}_{BEnc}}), \quad (4)$$

where $W_{\mathcal{P}_{BEnc}}$ denotes the trainable parameters. We concatenate the latent features \mathcal{A}_{BEnc} and \mathcal{P}_{BEnc} from the two encoder blocks and pass it through an LSTM to generate the beat-aware latent representation $h_{BEnc} \in \mathbb{R}_{BEnc}^H$ from the LSTM hidden states, H_{BEnc} being the latent dimension, as

$$\langle \text{LSTM o/p} \rangle, h_{BEnc} = \text{LSTM}_{BEnc}([\mathcal{A}_{BEnc}; \mathcal{P}_{BEnc}]; W_{L_{BEnc}}), \quad (5)$$

where $W_{L_{BEnc}}$ denotes the trainable parameters.

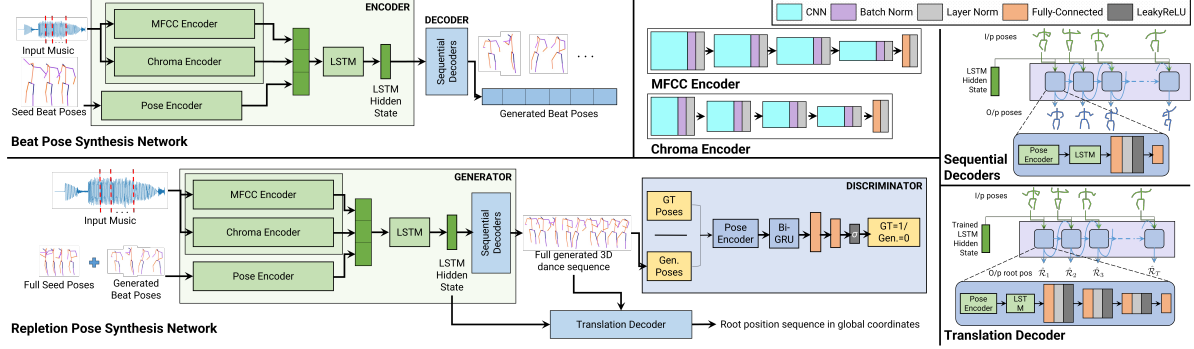


Figure 2: **DanceAnyWay Network Architecture.** Our network consists of two stages, Beat Pose Synthesis (BPS) and Repletion Pose Synthesis (RPS), trained one after the other. BPS (*top row, left*) has a seq-to-seq architecture, taking in the audio and a sequence of seed beat poses and generating all the beat poses. RPS (*bottom row, left*) has a generative adversarial architecture, taking in the audio, the seed poses, and the generated beat poses from BPS and generating the remaining poses to complete the dance sequence. Once fully trained, we use RPS to predict the root translations in the global coordinates using our translation decoder (*bottom row, right*). For completeness, we also show the architectures of our MFCC and Chroma encoders (*top row, middle*), which have the same architecture but with different layer sizes, and our sequential decoders (*top row, right*), which are architecturally similar to our translation decoder.

3.1.2 Decoder

We use sequential decoders to generate the beat poses corresponding to \mathcal{U}_{-B_S} one at a time. At each beat frame $f_b \in -B_S$ starting from the second, a decoder computes a latent representation $\mathcal{P}_{f_{b-1}}$ of the generated previous beat pose (ground-truth in case of the second beat frame) as

$$\mathcal{P}_{f_{b-1}} = \text{PoseEncoder}_{f_{b-1}} \left(\mathcal{U}_{f_{b-1}}; W_{P_{f_{b-1}}} \right), \quad (6)$$

where $W_{P_{f_{b-1}}}$ denotes the trainable parameters. It passes $\mathcal{P}_{f_{b-1}}$ through an LSTM to output features $o_{f_{b-1}} \in \mathbb{R}_{BEnc}^H$ as

$$o_{f_{b-1}}, \langle \text{LSTM hidden states} \rangle = \text{LSTM}_{f_{b-1}} \left(\mathcal{P}_{f_{b-1}}; W_{L_{f_{b-1}}} \right), \quad (7)$$

where $W_{L_{f_{b-1}}}$ denotes the trainable parameters. We linearly combine $o_{f_{b-1}}$ with the encoder latent representation h_{BEnc} to produce latent features $h_{f_{b-1}} \in \mathbb{R}_{BEnc}^H$ as

$$h_{f_{b-1}} = \gamma_{BEnc} h_{BEnc} + \gamma_{BDec} o_{f_{b-1}}, \quad (8)$$

where γ_{BEnc} and γ_{BDec} are fixed, non-trainable weights denoting the relevance of the combined audio and the seed beat poses, and the previous pose at frame f_{b-1} , in generating the current pose at frame f_b . To complete the decoder, we use a set of fully-connected (FC) layers to obtain the generated pose $\hat{\mathcal{U}}_{f_b} \in \mathbb{R}^{(J-1) \times 3}$ as

$$\hat{\mathcal{U}}_{f_b} = \text{FC}_{f_{b-1}} \left(h_{f_{b-1}}; W_{FC_{f_{b-1}}} \right), \quad (9)$$

where $W_{FC_{f_{b-1}}}$ denotes the trainable parameters. Using the decoders at all the beat frames, we generate the full beat pose sequence $\hat{\mathcal{U}}_{-B_S} = \left\{ \hat{\mathcal{U}}_{f_b} \right\}_{f_b \in -B_S}$.

3.2. Repletion Pose Synthesis

In contrast to our BPS network, which generates a sparse sequence of beat poses, our Repletion Pose Synthesis (RPS) network generates a dense sequence of repletion poses, capturing the finer details. Based on our experiments, a similar sequence-to-sequence architecture as that of the BPS fails to capture these details and tends to regress the sequences to mean poses. To overcome this issue and generate realistic dance motions, we opt for a generative adversarial architecture for our RPS, consisting of a generator and a discriminator. The generator takes in the raw audio waveform ψ of the input audio, the full seed pose sequence \mathcal{U}_S , and all the generated beat poses $\hat{\mathcal{U}}_{-B_S}$, and learns to generate the repletion poses $\hat{\mathcal{U}}_R$. The discriminator takes in the ground truth and generates full dance sequences $\mathcal{U} = \{\mathcal{U}_f\}_{f \in \{1, \dots, T\}}$ and $\hat{\mathcal{U}} = \{\hat{\mathcal{U}}_f\}_{f \in \{1, \dots, T\}}$ respectively and learns to classify them into different classes based on the physiological features of their movements. When we train the generator and the discriminator in tandem, the generator eventually learns to generate dance motions that the discriminator cannot distinguish from the ground truth, therefore leading to synthesized, plausible dance motions. Subsequently, we use a translation decoder that takes in the dance sequences from the fully trained generator and predicts the corresponding global root translations.

3.2.1 Generator

The generator follows an encoder-decoder architecture similar to that of BPS. Specifically, it consists of encoders for MFCC, Chroma CENS, pose features, and a decoder to gen-

erate the dance motions. The MFCC encoder takes in the MFCCs and their first- and second-order derivatives and uses convolutional layers to learn D_M -dimensional latent feature sequences $\mathcal{A}_{MREnc} \in \mathbb{R}^{D_M \times T}$ from their localized inter-dependencies as

$$\mathcal{A}_{MREnc} = \text{MFCCEncoder}_{REnc}(\text{MFCC}(\psi); W_{MREnc}), \quad (10)$$

where W_{MREnc} denotes the trainable parameters. The Chroma encoder takes in the Chroma CENS features and transforms them into D_{CREnc} -dim. latent feature sequences $\mathcal{A}_{CREnc} \in \mathbb{R}^{D_{CREnc} \times T}$ as

$$\mathcal{A}_{CREnc} = \text{ChromaEncoder}_{REnc}(\text{Chroma}(\psi); W_{CREnc}), \quad (11)$$

where W_{CREnc} denotes the trainable parameters. We have $D_{CREnc} > D_{CBEnc}$ to capture more latent features compared to BPS to help in generating the finer details in the repletion poses. We concatenate these two features into our audio features \mathcal{A}_{REnc} as

$$\mathcal{A}_{REnc} = [\mathcal{A}_{MREnc}; \mathcal{A}_{CREnc}] \in \mathbb{R}^{D_{\mathcal{A}_{REnc}} \times T}, \quad (12)$$

where $D_{\mathcal{A}_{REnc}} = D_M + D_{CREnc}$. The pose encoder takes in the concatenated seed poses \mathcal{U}_S and generated beat poses $\hat{\mathcal{U}}_{-BS}$ and outputs latent pose features $\mathcal{P} \in \mathbb{R}^{D_P \times T}$ as

$$\mathcal{P}_{REnc} = \text{PoseEncoder}_{REnc}([\mathcal{U}_S; \hat{\mathcal{U}}_{-BS}]; W_{PREnc}), \quad (13)$$

where W_{PREnc} denotes the trainable parameters. We concatenate the latent features \mathcal{A}_{REnc} and \mathcal{P}_{REnc} from the two encoder blocks and pass it through an LSTM to generate the beat-aware latent representation $h_{REnc} \in \mathbb{R}^{H_{REnc}}$ from the LSTM hidden states, H_{REnc} being the latent dimension, as

$$\langle \text{LSTM o/p} \rangle, h_{REnc} = \text{LSTM}_{REnc}([\mathcal{A}_{REnc}; \mathcal{P}_{REnc}]; W_{LREnc}), \quad (14)$$

where W_{LREnc} denotes the trainable parameters.

To generate the repletion poses corresponding to \mathcal{U}_R , we use sequential decoders similar to BPS. At each frame, $f \in 2, \dots, T$, a decoder computes a latent representation \mathcal{P}_{f-1} from the generated previous pose (ground-truth in case of the second frame) as

$$\mathcal{P}_{f-1} = \text{PoseEncoder}_{f-1}(\mathcal{U}_{f-1}; W_{P_{f-1}}), \quad (15)$$

where $W_{P_{f-1}}$ denotes the trainable parameters. It passes \mathcal{P}_{f-1} through an LSTM to output features $o_{f-1} \in \mathbb{R}^{H_{REnc}}$, as

$$o_{f-1}, \langle \text{LSTM hidden states} \rangle = \text{LSTM}_{f-1}(\mathcal{P}_{f-1}; W_{L_{f-1}}), \quad (16)$$

where $W_{L_{f-1}}$ denotes the trainable parameters. We linearly combine o_{f-1} with the encoder latent representation h_{REnc} to produce latent features $h_{f-1} \in \mathbb{R}^{H_{REnc}}$ as

$$h_{f-1} = \gamma_{REnc} h_{REnc} + \gamma_{RDec} o_{f-1}, \quad (17)$$

where γ_{REnc} and γ_{RDec} are fixed, non-trainable weights denoting the relevance of the combined audio and the seed poses, and the previous pose at frame $f-1$, in generating the current pose at frame f . To complete the decoder, we use a set of FC layers to obtain the generated pose $\hat{\mathcal{U}}_f \in \mathbb{R}^{(J-1) \times 3}$ as

$$\hat{\mathcal{U}}_f = \text{FC}_{f-1}(h_{f-1}; W_{FC_{f-1}}), \quad (18)$$

where $W_{FC_{f-1}}$ denotes the trainable parameters. Using the decoders at all the frames, we generate the full pose sequence $\hat{\mathcal{U}} = \{\hat{\mathcal{U}}_f\}_{f \in \{1, \dots, T\}}$.

3.2.2 Discriminator

Our discriminator takes in 3D dance pose sequences $\tilde{\mathcal{U}} \in \mathbb{R}^{(J-1) \times 3 \times T}$, which can be either the ground-truth \mathcal{U} or the generated $\hat{\mathcal{U}}$, and leverages the same pose encoder architecture to learn latent pose features $\tilde{\mathcal{P}}_{disc} \in \mathbb{R}^{D_P \times T}$ based on the physiological variations in the dances, as

$$\tilde{\mathcal{P}}_{disc} = \text{PoseEncoder}_{disc}(\tilde{\mathcal{U}}; W_{P_{disc}}), \quad (19)$$

where $W_{P_{disc}}$ denotes the trainable parameters. It then uses a bidirectional GRU (BiGRU) of latent dimension H_{disc} to learn the temporal inter-dependencies in the pose features, followed by a set of FC layers to compress the features into scalar variables and a sigmoid function to compute binary class probabilities $p_{disc} \in [0, 1]$, as

$$p_{disc} = \sigma(\text{FC}_{disc}(\text{BiGRU}_{disc}(\tilde{\mathcal{P}}_{disc}; W_{L_{disc}}); W_{FC_{disc}})), \quad (20)$$

where we only consider the output of the BiGRU and not its hidden states, $W_{L_{disc}}$ and $W_{FC_{disc}}$ denote the trainable parameters, and $\sigma(\cdot)$ denotes the sigmoid function.

3.2.3 Translation Decoder

Our translation decoder is architecturally similar to the sequential decoders in the RPS generator. However, instead of 3D poses, it predicts the sequence of root positions in the global coordinates corresponding to $\mathcal{R} = \{\mathcal{R}_f\}_{f \in \{1, \dots, T\}} \in \mathbb{R}^{3 \times T}$. At each frame $f \in \{2, \dots, T\}$, a decoder computes a latent representation \mathcal{P}_{f-1} of the pose \mathcal{U}_{f-1} as

$$\mathcal{P}_{tr_{f-1}} = \text{PoseEncoder}_{tr_{f-1}}(\mathcal{U}_{f-1}; W_{P_{tr_{f-1}}}), \quad (21)$$

where $W_{P_{tr_{f-1}}}$ denotes the trainable parameters. It passes $\mathcal{P}_{tr_{f-1}}$ through an LSTM to output features $o_{tr_{f-1}} \in \mathbb{R}^{H_{REnc}}$, as

$$o_{tr_{f-1}}, \langle \text{LSTM hidden states} \rangle = \text{LSTM}_{tr_{f-1}}(\mathcal{P}_{tr_{f-1}}; W_{L_{tr_{f-1}}}), \quad (22)$$

Table 1: **Quantitative Evaluation on the AIST++ Dataset [30]**. † numbers reported from [41], * numbers re-computed on our trimmed AIST++ dataset. Underline denotes best performance among numbers reported from [41], **bold** denotes best performance on our trimmed AIST++ dataset.

Method	Motion Quality		Motion Diversity		BAS †
	FID _k ↓	FID _g ↓	MD _k †	MD _g †	
Ground-Truth*	-	-	9.58	7.62	0.260
[28]†	86.43	43.46	6.85	3.32	0.161
DanceNet [49]†	69.18	25.49	2.86	2.85	0.143
DanceRevolution [19]†	73.42	25.92	3.52	4.87	0.195
Bailando [41]†	<u>28.16</u>	<u>9.62</u>	<u>7.83</u>	<u>6.34</u>	<u>0.233</u>
FACT [29]*	14.00	9.63	3.16	4.72	0.252
<i>DanceAnyWay (Ours)*</i>	17.98	9.42	5.03	4.98	0.229

where $W_{L_{tr_{f-1}}}$ denotes the trainable parameters. We linearly combine $o_{tr_{f-1}}$ with the RPS generator encoder latent representation h_{REnc} to produce latent features $h_{tr_{f-1}} \in \mathbb{R}_{REnc}^H$ as

$$h_{tr_{f-1}} = \gamma_{REnc} h_{REnc} + \gamma_{RDec} o_{tr_{f-1}}. \quad (23)$$

To complete the decoder, we use a set of FC layers to obtain the root positions $\hat{\mathcal{R}}_f \in \mathbb{R}^3$ as

$$\hat{\mathcal{R}}_f = \text{FC}_{tr_{f-1}} \left(h_{tr_{f-1}}; W_{FC_{tr_{f-1}}} \right), \quad (24)$$

where $W_{FC_{tr_{f-1}}}$ denotes the trainable parameters. Using the decoders at all the frames, we generate the full root position sequence $\hat{\mathcal{R}} = \left\{ \hat{\mathcal{R}}_f \right\}_{f \in \{1, \dots, T\}}$.

4. Training and Testing

We detail the loss functions we use for training our network, the implementation details, and the testing procedure.

4.1. Training Loss Functions

We use pose motion and leg motion losses to first train our BPS, then use pose motion, leg motion, and generative adversarial losses to train our RPS, and finally, the root translation loss to train our translation decoder. We describe each of these losses below.

4.1.1 Pose Motion Loss \mathcal{L}_{pm}

This is a linear combination of a distance metric $d_{pose}(\cdot)$ between the ground truth and the generated 3D dance pose sequences and a distance metric $d_{vel}(\cdot)$ between the corresponding temporal velocities. It captures the overall correctness and smoothness of the generated pose sequences in both spatial and temporal aspects. We write it as

$$\mathcal{L}_{pm} = \lambda_{pose} d_{pose}(\mathcal{U}^{(GT)}, \mathcal{U}^{(gen)}) + \lambda_{vel} d_{vel}(\Delta_f \mathcal{U}^{(GT)}, \Delta_f \mathcal{U}^{(gen)}), \quad (25)$$

Table 2: **Quantitative Evaluation on the TikTok Dataset [20]**. **Bold** denotes best performance.

Method	Motion Quality		Motion Diversity		BAS †
	FID _k ↓	FID _g ↓	MD _k †	MD _g †	
Ground-Truth	-	-	4.56	5.68	0.293
FACT [29]	37.85	18.05	3.19	4.42	0.287
<i>DanceAnyWay (Ours)</i>	41.10	14.39	3.82	5.16	0.288

where the Δ_f operator denotes forward differences between adjacent frames in the sequence, and λ_{pose} and λ_{vel} are experimentally determined fixed weights. For BPS, we have $\mathcal{U}^{(GT)} = \mathcal{U}_{-BS}$ and $\mathcal{U}^{(gen)} = \hat{\mathcal{U}}_{-BS}$ and set both d_{pose} and d_{vel} to be the mean squared error (MSE). For RPS, we have $\mathcal{U}^{(GT)} = \mathcal{U}$ and $\mathcal{U}^{(gen)} = \hat{\mathcal{U}}$ and set both d_{pose} and d_{vel} to be the smooth ℓ_1 loss. For both BPS and RPS, we use $\lambda_{pose} = \lambda_{vel} = 1$.

4.1.2 Leg Motion Loss \mathcal{L}_{lm}

This is a linear combination of the position and velocity losses operating exclusively on the angles θ_{fs} and angular velocities ω_{fs} between the femur and the shin bones of both legs. It provides additional constraints on leg movements and reduces foot sliding artifacts. We write it as

$$\mathcal{L}_{lm} = \lambda_{pose} d_{pose}(\theta_{fs}^{(GT)}, \theta_{fs}^{(gen)}) + \lambda_{vel} d_{vel}(\omega_{fs}^{(GT)}, \omega_{fs}^{(gen)}), \quad (26)$$

where we use the smooth ℓ_1 loss for both d_{pose} and d_{vel} in both BPS and RPS, and set $\lambda_{pose} = 0.3$ and $\lambda_{vel} = 0.7$.

4.1.3 Generative Adversarial Losses

We use the conventional generator loss \mathcal{L}_{gen} and discriminator loss \mathcal{L}_{disc} to train the generator (Sec. 3.2.1) and discriminator (Sec. 3.2.2) respectively in our RPS. For completeness, we write them as

$$\mathcal{L}_{gen} = -\mathbb{E} \left[\log \left(\text{Disc}(\hat{\mathcal{U}}) \right) \right], \quad (27)$$

$$\mathcal{L}_{disc} = -\mathbb{E} \left[\log \left(\text{Disc}(\mathcal{U}) \right) \right] - \mathbb{E} \left[\log \left(1 - \text{Disc}(\hat{\mathcal{U}}) \right) \right], \quad (28)$$

where $\text{Disc}(\cdot)$ denotes our entire discriminator network.

4.1.4 Root Translation Loss \mathcal{L}_{rt}

This is a linear combination of the position and velocity losses operating exclusively on the sequences of root positions in the global coordinates. It ensures the correctness and smoothness of the trajectories generated by our transla-

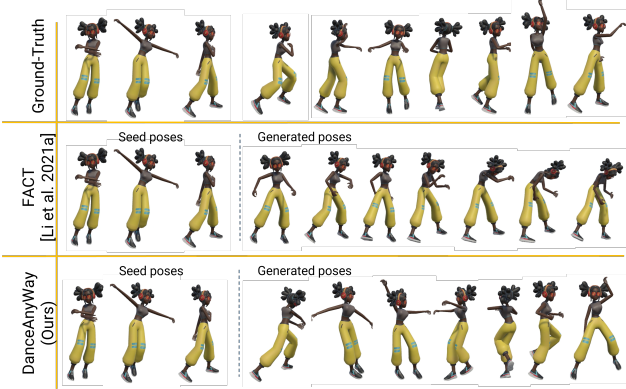


Figure 3: **Visualizations on the AIST++ Dataset [30].** We show sampled frames in a left-to-right sequence for one dance motion. Our generated samples show more diverse movements compared to FACT.

tion decoder (Sec. 3.2.3). We write it as

$$\mathcal{L}_{rt} = \lambda_{pose} d_{pose}(\mathcal{R}, \hat{\mathcal{R}}) + \lambda_{vel} d_{vel}(\Delta_f \mathcal{R}, \Delta_f \hat{\mathcal{R}}), \quad (29)$$

where we use MSE for d_{pose} and the smooth ℓ_1 loss for d_{vel} , and set $\lambda_{pose} = \lambda_{vel} = 1$.

4.1.5 Total Training Loss for BPS and RPS Generator

For our BPS, we use the total loss \mathcal{L}_{BPS} as

$$\mathcal{L}_{BPS} = \lambda_{pm} \mathcal{L}_p m + \lambda_{lm} \mathcal{L}_{lm}, \quad (30)$$

and for our RPS generator, we use the total loss \mathcal{L}_{RPSGen} as

$$\mathcal{L}_{RPSGen} = \lambda_{pm} \mathcal{L}_p m + \lambda_{lm} \mathcal{L}_{lm} + \lambda_{gen} \mathcal{L}_{gen}, \quad (31)$$

where we experimentally set the weights $\lambda_{pm} = 5$, $\lambda_{lm} = 3e - 3$, and $\lambda_{gen} = 5e - 2$.

4.2. Implementation Details

We train our full network in three sequential stages: BPS, followed by RPS, followed by our translation decoder. We train our network using 10-second dance clips sampled at 10 fps, *i.e.*, we have $T = 100$. We use a seed pose sequence length $T_S = 20$. We use the method of [33] to extract MS COCO keypoints with $J = 18$ body joints from videos. We use the Librosa library [7] to extract the MFCC and the Chroma CENS features, and compute the beat frames. We use a maximum of $|B| = 20$ beat frames and $|B_S| = 3$ seed beat frames. We use $D_M = 32$, $D_{CBEnc} = 4$, $D_{CREnc} = 6$, $D_P = 16$, $H_{BEnc} = 256 \times 3$, $H_{REnc} = 256 \times 5$, and $H_{disc} = 64 \times 4$. For training our BPS, we experimentally set the hyperparameters $\gamma_{BEnc} = 0.3$ and $\gamma_{BDec} = 0.7$.

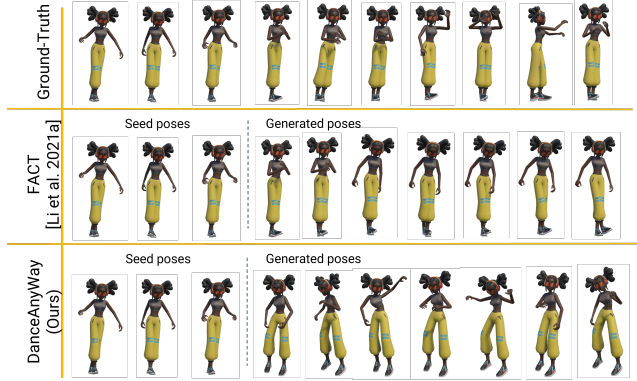


Figure 4: **Visualizations on the TikTok Dataset [20].** We show sampled frames in a left-to-right sequence for one dance motion. FACT outputs tend to regress to mean configurations, whereas our method continues to generate plausible motions.

We use the Adam optimizer [22] with a mini-batch size of 8, an initial learning of $1e - 3$ that we drop to $1e - 4$ after 700 epochs, and train for a total of 1,000 epochs. For training our RPS, we experimentally set the hyperparameters $\gamma_{REnc} = 0.4$ and $\gamma_{RDec} = 0.6$. We use the Adam optimizer [22] with a mini-batch size of 8 for both the generator and the discriminator, a learning rate of $1e - 3$ for the generator, a learning rate of $1e - 5$ for the discriminator, and train for a total of 600 epochs. Lastly, we train our translation decoder using the Adam optimizer [22] with a mini-batch size of 8, an initial learning rate of $5e - 4$ that we drop to $1e - 4$ after 450 epochs, and train for a total of 800 epochs. Training our BPS, RPS, and translation decoder takes 40, 72, and 24 hours respectively, on an Nvidia RTX 2060 GPU.

4.3. Testing

At test time, we provide the input audio and the seed poses to our network. Our BPS takes in the audio and the seed beat poses to generate the remaining beat poses. Our RPS uses the audio, the seed poses, and the BPS-generated beat poses to generate the full dance sequences. Our translation decoder takes in the generated dance sequences to predict the global root translations.

5. Experiments and Results

We train and test our network on two datasets, one for single-genre dances and one for mixed-genre dances. We describe these datasets and our quantitative and qualitative evaluations.

Table 3: **User Study Scores.** We report the mean preferences on samples generated from the AIST++ dataset [30] in the left column and mean Likert-scale scores on samples generated from the TikTok dataset [20] in the right column.

AIST++		TikTok	
Mean Preferences (%)		Mean Likert Scores (out of 5)	
Neither	15.91	Ground-Truth	2.23
FACT [29]	37.50	FACT [29]	1.91
<i>DanceAnyWay (Ours)</i>	46.59	<i>DanceAnyWay (Ours)</i>	2.54

5.1. Datasets

For evaluating our method on single-genre dances, we use the AIST++ dataset [30], which is a large-scale 3D human motion dance dataset consisting of (music, keypoints) sample pairs spanning ten different dance genres. For our experiments, we drop samples that are less than 10 seconds long. We use 447 training samples and 67 testing samples from the dataset. For evaluating on mixed-genre dances, we use the TikTok dataset introduced by [20]. This dataset contains short dance videos posted on the TikTok social media platform. For our work, we extract 3D keypoints from the dance videos using the method of [33] to prepare the (music, keypoints) pairs. We use 151 samples in the train set and 35 samples in the test set such that there is no overlapping music or dancer between the train and the test sets.

5.2. Evaluation Metrics

We use the same three metrics reported by [29]: Fréchet Inception Distance (FID) on the kinetic (k) and geometric (g) features computed from the ground-truth and the generated dances, Motion Diversity (MD) on the same kinetic and geometric features between all the generated dances, and the Beat Alignment Score (BAS) between the audio and the motion beats.

5.3. Quantitative Evaluation

We compare our proposed method, DanceAnyWay, with the baseline methods of [28], DanceNet [49], DanceRevolution [19], FACT [29], and Bailando [41] on the AIST++ dataset [30]. We report the performance of all these methods in Table 1. Of these methods, we pick FACT [29] as the best method with available open-source code and compare with it on the TikTok dataset [20] in Table 2. We observe that the performance of our method is comparable to the best baselines on all the metrics on the single-genre AIST++ dataset, and is better than the baseline of FACT on the mixed-genre TikTok dataset. Specifically, we note that compared to the best available baseline of FACT [29], our FID_g scores are about 2% better on both the datasets, and our MD_k and MD_g scores are about 5.9% and 5.5% bet-

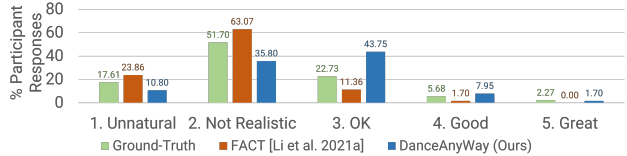


Figure 5: **Plausibility scores on the TikTok Dataset [20].** Distributions of the Likert-scale scores for the three candidates on the TikTok dataset.

ter on the AIST dataset and about 2.0% and 1.6% better on the TikTok dataset. We note the higher FID_k values of our method on both datasets, indicating that our method has learned different motion variations and, therefore, different kinetic features compared to the ground-truth. Lastly, we note that our BAS is within 10% of that of FACT on the AIST++ dataset and 0.3% better than FACT on the TikTok dataset. These results demonstrate the benefit of our two-stage approach in generating mixed-genre dance motions.

5.4. Qualitative Results

To render our generation 3D motions on human models, we retarget our MS COCO keypoints to the SMPL format [31] and follow the approach of [29] to apply them on Mixamo characters [34]. We show sampled frames generated by FACT [29] and by our method from one dance motion each from the AIST++ dataset [30] and the TikTok dataset [20] in Fig. 3 and Fig. 4 respectively. We can observe that the dance motions of our method are more animated and diverse. We show full video results of dance motions from both these datasets in our supplementary material.

5.5. User Study

We evaluate the perceived performance of our generated dance motions through a two-part user study on the two datasets, AIST++ [30] for single-genre dances and TikTok [20] for mixed-genre dances. In the first part, we randomly selected four samples from the AIST++ test set. We showed the participant a pair of randomly ordered dances for each of the four samples, one generated by FACT [29] and the other generated by our method. We asked the participant to mark which of the two dances they preferred for each audio based on the motion quality and diversity. We excluded the corresponding ground-truth AIST++ dances in this part as those were recorded by professionals and were visually superior to all the generated dances in obvious ways. In the second part, we randomly selected four samples from the TikTok test set. We showed the participant three randomly ordered dances for each of the four samples, the ground-truth, one generated by FACT [29], and one generated by our method. We asked the participant to mark the plausibility (based on motion quality and diversity) of each

of the three dances on the five-point Likert scale, with 1 being the worst and 5 being the best.

A total of 44 participants responded to our user study. We report the mean percentage of participant preferences for the two candidates in the first part in the left column of Table 3. We note that, on average, participants preferred our generated dance motions 9% more over those of FACT. We report the mean Likert-scale scores for the three candidates in the second part in the right column of Table 3 and the score distributions in Fig. 5. We note that our mean score is about 0.6 (or 12% w.r.t. the Likert-scale range of 5) higher than that of FACT (and even 0.3 or 6% better than the rendered ground-truth), indicating better plausibility for our method. We also note that the mean scores are quite low, which follows the general feedback from the participants that the leg motions were improbable in most cases. This is a consequence of the nature of the TikTok dataset, where the lower body is either off-camera or occluded in many samples, thus leading to poor keypoint extraction and, by extension, poor learning of the lower-body motions. Lastly, we note that while our FID_k and BAS scores (Tables 1 and 2) were poorer or almost identical to that of FACT, those did not correspond to visual artifacts that affected the participants’ responses, indicating that those scores may not sufficiently capture the perceived quality of dance motions.

6. Conclusion, Limitations and Future Work

We have presented a novel learning method to synthesize mixed-genre 3D dance motions from music or song audio. Our method works in two hierarchical stages, first generating the beat poses given the audio and then generating the remaining poses given both the audio and the beat poses. Through extensive quantitative and qualitative evaluations and a user study, we have demonstrated the state-of-the-art performance of our method on both single-genre and mixed-genre datasets. However, our work also has some limitations. First, we do not explicitly consider various dance styles or genres but implicitly learn them based on the audio and our beat pose synthesis network. We can extend our method to incorporate labels for different dance styles to make the dance generation more controllable. We also do not consider physical constraints based on the dancers’ capabilities and interactions with their environments, such as the floor and dancing props, which are exciting future directions to pursue.

References

[1] Emre Aksan, Manuel Kaufmann, Peng Cao, and Otmar Hilliges. A spatio-temporal transformer for 3d human motion prediction. 2020. 2

[2] Emre Aksan, Manuel Kaufmann, and Otmar Hilliges. Structured prediction helps 3d human motion modelling. 2019

IEEE/CVF International Conference on Computer Vision (ICCV), pages 7143–7152, 2019. 2

[3] Omid Alemi, Jules Franoise, and Philippe Pasquier. Groovenet: Real-time music-driven dance movement generation using artificial neural networks. *networks*, 8(17):26, 2017. 2

[4] Okan Arıkan and D.A. Forsyth. Interactive motion generation from examples. *Proceedings of the 29th annual conference on Computer graphics and interactive techniques*, 2002. 2

[5] Uttaran Bhattacharya, Elizabeth Childs, Nicholas Rewkowski, and Dinesh Manocha. Speech2affectivegestures: Synthesizing co-speech gestures with generative adversarial affective expression learning. In *Proceedings of the 29th ACM International Conference on Multimedia*, MM ’21, New York, NY, USA, 2021. Association for Computing Machinery. 3

[6] Uttaran Bhattacharya, Nicholas Rewkowski, Abhishek Banerjee, Pooja Guhan, Aniket Bera, and Dinesh Manocha. Text2gestures: A transformer-based network for generating emotive body gestures for virtual agents. In *2021 IEEE Virtual Reality and 3D User Interfaces (VR)*. IEEE, mar 2021. 2

[7] Brian McFee, Colin Raffel, Dawen Liang, Daniel P.W. Ellis, Matt McVicar, Eric Battenberg, and Oriol Nieto. librosa: Audio and Music Signal Analysis in Python. In Kathryn Huff and James Bergstra, editors, *Proceedings of the 14th Python in Science Conference*, pages 18 – 24, 2015. 7

[8] Judith Butepage, Michael J. Black, Danica Kragic, and Hedvig Kjellstrom. Deep representation learning for human motion prediction and classification. In *2017 IEEE Conference on Computer Vision and Pattern Recognition (CVPR)*, pages 1591–1599, 2017. 2

[9] Xiaoxiao Du, Ram Vasudevan, and Matthew Johnson-Roberson. Bio-1stm: A biomechanically inspired recurrent neural network for 3-d pedestrian pose and gait prediction. *IEEE Robotics and Automation Letters*, 4(2):1501–1508, 2019. 2

[10] Makeda Easter. *Rise of The Dancefluencer*, 2020. 2

[11] Rukun Fan, Songhua Xu, and Weidong Geng. Example-based automatic music-driven conventional dance motion synthesis. *IEEE Transactions on Visualization and Computer Graphics*, 18(3):501–515, 2012. 2

[12] Ylva Ferstl, Michael Neff, and Rachel McDonnell. Multi-objective adversarial gesture generation. In *Motion, Interaction and Games*, MIG ’19, New York, NY, USA, 2019. Association for Computing Machinery. 3

[13] Katerina Fragkiadaki, Sergey Levine, Panna Felsen, and Jitendra Malik. Recurrent network models for human dynamics. *2015 IEEE International Conference on Computer Vision (ICCV)*, pages 4346–4354, 2015. 2

[14] Aphrodite Galata, Neil Johnson, and David Hogg. Learning variable-length markov models of behavior. *Computer Vision and Image Understanding*, 81(3):398–413, 2001. 2

[15] Partha Ghosh, Jie Song, Emre Aksan, and Otmar Hilliges. Learning human motion models for long-term predictions. In *2017 International Conference on 3D Vision (3DV)*, pages 458–466, 2017. 2

- [16] Shiry Ginosar, Amir Bar, Gefen Kohavi, Caroline Chan, Andrew Owens, and Jitendra Malik. Learning individual styles of conversational gesture. In *Proceedings of the IEEE/CVF Conference on Computer Vision and Pattern Recognition (CVPR)*, June 2019. 2
- [17] Daniel Holden, Jun Saito, and Taku Komura. A deep learning framework for character motion synthesis and editing. *ACM Trans. Graph.*, 35(4), jul 2016. 2
- [18] Daniel Holden, Jun Saito, Taku Komura, and Thomas Joyce. Learning motion manifolds with convolutional autoencoders. In *SIGGRAPH Asia 2015 Technical Briefs*, SA '15, New York, NY, USA, 2015. Association for Computing Machinery. 2
- [19] Ruozi Huang, Huang Hu, Wei Wu, Kei Sawada, Mi Zhang, and Daxin Jiang. Dance revolution: Long-term dance generation with music via curriculum learning. In *9th International Conference on Learning Representations, ICLR 2021, Virtual Event, Austria, May 3-7, 2021*. OpenReview.net, 2021. 6, 8
- [20] Yasamin Jafarian and Hyun Soo Park. Learning high fidelity depths of dressed humans by watching social media dance videos. In *Proceedings of the IEEE/CVF Conference on Computer Vision and Pattern Recognition (CVPR)*, pages 12753–12762, June 2021. 2, 6, 7, 8
- [21] Ashesh Jain, Amir Roshan Zamir, Silvio Savarese, and Ashutosh Saxena. Structural-rnn: Deep learning on spatio-temporal graphs. *2016 IEEE Conference on Computer Vision and Pattern Recognition (CVPR)*, pages 5308–5317, 2015. 2
- [22] Diederik P. Kingma and Jimmy Ba. Adam: A method for stochastic optimization, 2014. 7
- [23] Lucas Kovar, Michael Gleicher, and Frédéric Pighin. Motion graphs. In *ACM SIGGRAPH 2008 Classes*, SIGGRAPH '08, New York, NY, USA, 2008. Association for Computing Machinery. 2
- [24] Hsu kuang Chiu, Ehsan Adeli, Borui Wang, De-An Huang, and Juan Carlos Niebles. Action-agnostic human pose forecasting. *2019 IEEE Winter Conference on Applications of Computer Vision (WACV)*, pages 1423–1432, 2018. 2
- [25] Taras Kucherenko, Patrik Jonell, Sanne van Waveren, Gustav Eje Henter, Simon Alexandersson, Iolanda Leite, and Hedvig Kjellström. Gesticulator: A framework for semantically-aware speech-driven gesture generation. *ICMI '20*, page 242–250, New York, NY, USA, 2020. Association for Computing Machinery. 2
- [26] Kimerer LaMothe. The dancing species: how moving together in time helps make us human. *Aeon*, June, 1, 2019. 1
- [27] Hsin-Ying Lee, Xiaodong Yang, Ming-Yu Liu, Ting-Chun Wang, Yu-Ding Lu, Ming-Hsuan Yang, and Jan Kautz. Dancing to music. In H. Wallach, H. Larochelle, A. Beygelzimer, F. d'Alché-Buc, E. Fox, and R. Garnett, editors, *Advances in Neural Information Processing Systems*, volume 32. Curran Associates, Inc., 2019. 2
- [28] Jiaman Li, Yihang Yin, Hang Chu, Yi Zhou, Tingwu Wang, Sanja Fidler, and Hao Li. Learning to generate diverse dance motions with transformer, 2020. 2, 6, 8
- [29] R. Li, S. Yang, D. A. Ross, and A. Kanazawa. Ai choreographer: Music conditioned 3d dance generation with aist++. *2021 IEEE/CVF International Conference on Computer Vision (ICCV)*, pages 13381–13392, Los Alamitos, CA, USA, oct 2021. IEEE Computer Society. 2, 6, 8
- [30] Ruilong Li, Shan Yang, David A. Ross, and Angjoo Kanazawa. Learn to dance with aist++: Music conditioned 3d dance generation, 2021. 2, 6, 7, 8
- [31] Matthew Loper, Naureen Mahmood, Javier Romero, Gerard Pons-Moll, and Michael J. Black. SMPL: A skinned multi-person linear model. *ACM Trans. Graphics (Proc. SIGGRAPH Asia)*, 34(6):248:1–248:16, Oct. 2015. 8
- [32] S. Mascarenhas, M. Guimarães, R. Prada, J. Dias, P. A. Santos, K. Star, B. Hirsh, E. Spice, and R. Kommeren. A virtual agent toolkit for serious games developers. In *2018 IEEE Conference on Computational Intelligence and Games (CIG)*, pages 1–7, 2018. 2
- [33] Dushyant Mehta, Oleksandr Sotnychenko, Franziska Mueller, Weipeng Xu, Srinath Sridhar, Gerard Pons-Moll, and Christian Theobalt. Single-shot multi-person 3d pose estimation from monocular rgb. In *2018 International Conference on 3D Vision (3DV)*, pages 120–130, 2018. 7, 8
- [34] Mixamo. Mixamo. 2008. 1, 8
- [35] K. S. R. Murty and B. Yegnanarayana. Combining evidence from residual phase and mfcc features for speaker recognition. *IEEE Signal Processing Letters*, 13(1):52–55, 2006. 3
- [36] Daniel Neiberg, Kjell Elenius, and Kornel Laskowski. Emotion recognition in spontaneous speech using gmms. In *Ninth international conference on spoken language processing*, 2006. 3
- [37] Oculus. *Facebook Horizon*, <https://www.oculus.com/facebook-horizon/>, 2021. 2
- [38] K. Pullen and C. Bregler. Animating by multi-level sampling. In *Proceedings Computer Animation 2000*, pages 36–42, 2000. 2
- [39] Alejandro Hernandez Ruiz, Juergen Gall, and Francesc Moreno-Noguer. Human motion prediction via spatio-temporal inpainting. *2019 IEEE/CVF International Conference on Computer Vision (ICCV)*, pages 7133–7142, 2018. 2
- [40] Takaaki Shiratori, Atsushi Nakazawa, and Katsushi Ikeuchi. Dancing-to-music character animation. *Computer Graphics Forum*, 25(3):449–458, 2006. 2
- [41] Li Siyao, Weijiang Yu, Tianpei Gu, Chunze Lin, Quan Wang, Chen Qian, Chen Change Loy, and Ziwei Liu. Bailando: 3d dance generation by actor-critic gpt with choreographic memory. In *Proceedings of the IEEE/CVF Conference on Computer Vision and Pattern Recognition (CVPR)*, pages 11050–11059, June 2022. 2, 6, 8
- [42] Statista. Statista. 2020. 1
- [43] Taoran Tang, Jia Jia, and Hanyang Mao. Dance with melody: An lstm-autoencoder approach to music-oriented dance synthesis. In *Proceedings of the 26th ACM International Conference on Multimedia*, MM '18, page 1598–1606, New York, NY, USA, 2018. Association for Computing Machinery. 2
- [44] Borui Wang, Ehsan Adeli, Hsu kuang Chiu, De-An Huang, and Juan Carlos Niebles. Imitation learning for human pose prediction. *2019 IEEE/CVF International Conference on Computer Vision (ICCV)*, pages 7123–7132, 2019. 2

- [45] Katie Watson, Samuel S. Sohn, Sasha Schriber, Markus Gross, Carlos Manuel Muniz, and Mubbasir Kapadia. Storyprint: An interactive visualization of stories. In *Proceedings of the 24th International Conference on Intelligent User Interfaces, IUI '19*, page 303–311, New York, NY, USA, 2019. Association for Computing Machinery. [2](#)
- [46] Nelson Yalta, Shinji Watanabe, Kazuhiro Nakadai, and Tetsuya Ogata. Weakly supervised deep recurrent neural networks for basic dance step generation, 2018. [2](#)
- [47] Sijie Yan, Zhizhong Li, Yuanjun Xiong, Huahan Yan, and Dahua Lin. Convolutional sequence generation for skeleton-based action synthesis. In *2019 IEEE/CVF International Conference on Computer Vision (ICCV)*, pages 4393–4401, 2019. [2](#)
- [48] Youngwoo Yoon, Bok Cha, Joo-Haeng Lee, Minsu Jang, Jaeyeon Lee, Jaehong Kim, and Geehyuk Lee. Speech gesture generation from the trimodal context of text, audio, and speaker identity. *ACM Transactions on Graphics*, 39(6), 2020. [3](#)
- [49] Wenlin Zhuang, Congyi Wang, Jinxiang Chai, Yangang Wang, Ming Shao, and Siyu Xia. Music2dance: Dancenet for music-driven dance generation. 18(2), feb 2022. [2](#), [6](#), [8](#)